FLEXURAL AND SHEAR CAPACITY OF PRC BEAMS DAMAGED BY COMBINED DETERIORATION DUE TO ASR AND CORROSION

Yasuhiro Mikata [1*], Yoshinori Shimazu[2], Yuji Hatano[3], Susumu Inoue[1]

[1]Osaka Institute of Technology, Osaka, JAPAN

[2]Central Nippon Highway Engineering Tokyo Company, Tokyo, JAPAN

[3]JIP Techno Science Corporation, Osaka, JAPAN

Abstract

It is important to clarify the residual performance of the loading capacity of reinforced concrete and prestressed concrete members damaged by ASR. Especially, the loading capacity performance of the prestressed concrete beams, which have reinforcing steel bar fractures, is not known. In this study, prestressed concrete beams, which are damaged by combined deterioration and have steel bar fractures, are tested to evaluate the shear capacity and flexural capacity. From these results, when specimen has a fractured anchorage under the condition of the shear reinforcement due to ASR, if the development length of shear reinforcement is satisfied to shear crack, shear reinforcement is performed effectively. However, when specimen has a fractured anchorage and is corroded due to combined deterioration of ASR and corrosion, performance of the shear reinforcement is decreased.

Keywords: Fractured reinforcing steel bars, Deterioration of bond strength, loading capacity, Residual performance, PC beams

1 INTRODUCTION

Instances of reinforcing steel fracture in concrete structures damaged by alkali-silica reaction (ASR) have been discovered recently. Japan currently counts some 30 ASR-damaged structures, including highway and railroad bridges, confirmed to have steel bar fractures [1]. Fractured reinforcing steel bars were found at some corners of the hoop reinforcements. It is assumed that reinforcing steel bars were fractured on account of the expansion pressure resulting from ASR. Andesite type reactive aggregate, which is very prone to volume expansion, was used as the concrete material at the locations where these steel fractures occurred.

The safety of a structure is considered not to be seriously compromised [2]. However, the safety of a structure becomes questionable when the confinement of concrete becomes degraded due to fracture of reinforcing steel bars. When many steel bars are fractured, strengthening is often required because of the problem of possible over-loading caused by the reduced performance of the member or structure due to weakened concrete strength and reduced modulus of elasticity caused by steel confinement fractures.

In such a situation, it is important to clarify the residual performance of the loading capacity of reinforced concrete [3,4] and prestressed concrete members [5] damaged by ASR. Especially, the loading capacity performance of the prestressed concrete beams, which have reinforcing steel bar fractures, is not

* Correspondence to: mikata@civil.oit.ac.jp

known. In this study, prestressed concrete beams, which are damaged by combined deterioration and have steel bar fractures, are tested to evaluate the shear capacity and flexural capaxcity.

2 MEASUREMENT AND TEST METHOD

2.1 Test variables

Details of these test variables are shown in Table 5. Properties of concrete are shown in Table 1. Test specimens used are prestressed reinforced concrete (PRC)simple beams with rectangular section of 125× 250mm and total length of 1800mm as shown Fig 1. The specimens are PRC beams with deformed mild steel D16 bars(f_{sy}=331N/mm^2)for the longitudinal non-tensioned reinforcement and D6(f_{sy}=432N/mm^2)for shear reinforcement. As for prestressing steel, prestressing bars of ϕ =17mm(f_{py}=1000N/mm^2)were used.

The test variables are as follows:

(1)Deterioration type: ASR (A-series specimens), Combined deterioration due to ASR and corrosion (AC-series specimens), Sound (N-series specimen)

(2)The condition of shear reinforcement: fractured anchorage (fractured reinforcing steel bar due to ASR is simulated) , sound.

(3)Spacing of shear reinforcement: s=150(shear reinforcement ratio ρ_w=0.34%), s=100(shear reinforcement rario ρ_w=0.51%)

(4) Stress at the extreme tension fiber of the section: σ_{ct}=2.0 N/mm^2 and 4.0 N/mm^2

In the case of all specimens, calculation of ultimate shear capacity is smaller than that of ultimate flexural capacity. It is assumed that shear failure is occurred after yielding longitudinal reinforcements and prestressing bars are not yield.

Mix proportion of concrete is show in table 2. The equivalent alkali content was 11.59kg/m^3 using NaCl. The main reactive components identified in texture of andesite crushed stone were a volcanic glass, cristobalite and tridymite.

In the A-series specimens, All specimens were cured for 4weeks under normal moist-curing at 20℃ . After 4 weeks of curing, they were placed in temperate humidity chamber to progress ASR for 365days under high temperate(40℃) and high humidity (90%).

In the AC-series specimens, All specimens were cured for 4weeks under normal moist-curing at 20℃ . After 4 weeks of curing, they were placed in temperate humidity chamber to progress ASR for 365days under high temperate(40℃) and high humidity (90%). They are sprayed with 3% saline water from 715days to loading test (1088days) for every week days.

2.2 Measurements of ASR expansion

Contact gauge tip was attached in both sides of tests piece specimens and beam specimens to measure ASR expansion. ASR expansion of tests piece specimens are evaluated free expansion without reinforcement. Expansion strain of beam specimens are measured in surface concrete on the position of longitudinal reinforcement (the length of extreme compression fiber of the section 20mm and 210mm). Figure 1 shows the position of contact gauge tip for beam specimens.

2.3 Measurements of corrosion

The ratio of corrosion weight loss was calculated from the sound (original) weight of the reinforcement and the corrosion weight loss in the overall length. The sound (original) weight of the reinforcement was derived from measuring the reinforcement alone before casting the RC beam. The

corrosion weight loss was measured by removing the rust of corroded longitudinal reinforcement, which was taken out of RC beam after the loading test, using a 10% di-ammonium hydrogen citrate solution at 60°C.

2.4 Loading test

All specimens are tested under symmetrical two-point loading. The specimens have a total length of 1800mm, a flexural span of 300mm and a shear span of 550mm. The shear span-effective depth ratio of these beams are a/d=2.38. During the loading tests, the applied load, shear reinforcement strain and deflection at the center of the span are measured.

3 RESULTS

3.1 ASR expansion

Figure 2 shows the axial strain of ASR expansion for AC-series beam and A-1 specimens. ASR expansion strain of AC-1 is about 1000(μ) at 1088days. That of AC-2 is about 1500(μ). ASR expansion of AC-1 is smaller than that of AC-2. That of AC-1 is confined by sound shear reinforcement. However, in the case of AC-2, confining effect of shear reinforcement is decreased due to fractured anchorage of that. ASR expansion of AC-3 is smaller than that of AC-2. In the case of AC-3, confining effect for ASR expansion due to the introduced prestress is larger than that of AC-2.

In the A-series, Free Expansion strain of tests piece specimens was 4600(μ) at 365days. In the AC-series, Free Expansion strain of tests piece specimens was 4900(μ) at 715days.

3.2 Condition of crack

Figure 3 shows condition of crack before loading tests. Crack densities of specimens are listed in table 3. In the case of crack density, 1mm over width of crack of AC-1 is smaller than that of AC-2. That of AC-1 is confined by sound shear reinforcement. However, in the case of AC-2, confining effect of shear reinforcement is decreased due to fractured anchorage of that. Crack density of AC-3 is smaller than that of AC-2. Crack density decreases with increasing the introduced prestress. Crack width is decreased by the introduced prestress. Both ASR crack and corrosion crack are occurred in the AC-series specimens. Crack density of AC-series specimens is larger than that of A-series specimens. In the case of AC-series specimens, 1mm over width of crack is occurred in the surface concrete on the position of longitudinal reinforcement due to corrosion of reinforcement.

3.3 Measurements of corrosion

The ratio of corrosion weight loss, yield strength and Young's modulus are listed in table 4. The water to cement ratio of AC-series specimens is small relatively (45.5(%)). Therefore, the penetration of chloride ion for concrete is slow and the ratios of corrosion weight loss are small in AC- series specimens.

3.4 Failure mode

Figure 4 shows the final failure mode. All the specimens showed flexural tension failure. In these cases, the longitudinal reinforcements yielded and prestressing bars are not yielded. In the case of almost all the specimens except for beam A-4, the ultimate shear capacity is smaller than the ultimate flexural capacity. However, these beams did not show shear failure. Ultimate shear capacity is calculated by JSCE code [6]. Ultimate flexural capacity is calculated by fiber model. Calculation is used by test results of concrete strength at 1088 days. Calculation values of shear force carried by concrete are not evaluated chemical prestress.

On one hand, in the case of N-1, shear crack is occurred from loading point to support point in shear span. Finally, this beam is failed due to the compressive failure in flexural span and is showed flexural tension

failure. On the other hand, in the case of A-series specimens, shear crack is not occurred clearly. In the case of AC-1, shear crack is not occurred due to the sound anchorage of the shear reinforcement. In the case of AC-3, the bonding crack is occurred along the longitudinal reinforcement. In the case of AC-2 and AC-3, shear crack is occurred clearly compared with A-2 and A-3.

3.5 load and deflection

Figure 5 shows the relationship between load and deflection in AC-series and N-1. Figure 6 shows the relationship between load and deflection in AC-1, A-1 and N-1.

AC-2 has a fractured anchorage under the condition of the shear reinforcement. However, AC-2 and AC-1 are same behaviour in load and deflection. Ultimate load and initial stiffness of AC-3 are larger than that of AC-2. However, ductility of AC-3 is smaller than that of AC-2. Ultimate load and initial stiffness of AC-1, A-1 are larger than that of N-1. Ductility of AC-1 is smaller than that of A-1.

3.6 Strain of the shear reinforcement

Figure 7 shows the relationship between load and strain of the shear reinforcement. Figure 1 shows the position of strain gauge in the shear reinforcement. Strain of Figure 7 is average value in all strain gauges of each specimen. The sound (original) yield strain of shear reinforcement is 2160 (μ) and shear reinforcements are not yielded in all specimens.

In the case of N-1, strain occurred after shear cracking in shear reinforcement. However, strain of AC-1 did not occur clearly in shear reinforcement. In the case of AC-2, although shear cracking did occur, Strain did not occurred. Strain of AC-2 is smaller than that of A-2 and AC-1.

3.7 Shear crack width

Figure 8 shows the relationship between load and shear crack width. Figure 1 shows the position of crack gauge is the specimen.

In the case of N-1, shear crack width is increased after shear cracking. However, in the case of AC-1, shear crack width is not increased clearly. Shear crack width of AC-1 is smaller than that of N-1 due to chemical prestress of ASR. Shear crack width of AC-2 is larger than that of A-2 and AC-1.

4 DISCUSSION

4.1 Failure mode

On one hand, in the case of sound specimen (N-1), shear crack occurred from loading point to support point in shear span. Finally, this beam is failed due to the compressive failure in flexural span and is showed flexural tension failure. On the other hand, in the case of A-series specimens, shear crack is not occurred clearly. The shear force carried by concrete of A-series specimens is larger than that of N-1 specimens due to the chemical prestress of ASR. Therefore, shear crack is not occurred clearly.

In the case of AC-1, shear crack did not occurred due to the sound anchorage of the shear reinforcement. AC-2 has a fractured anchorage under the condition of the shear reinforcement. Therefore, shear cracking occurred due to decreasing the performance of the shear reinforcement.

In the case of AC-3, the bonding crack occurred along the longitudinal reinforcement. The confinement force of the dowel action of the longitudinal reinforcements is decreased due to fractured anchorage of the shear reinforcement. In the case of AC-2 and AC-3, shear cracking occurred clearly compared with A-2 and A-3. The bond strength between shear reinforcement and concrete is decreased due to corrosion of shear reinforcement. Therefore, the performance of the shear reinforcement is decreased.

4.2 Load and deflection General

Ultimate load and initial stiffness of AC-3 are larger than that of AC-2. However, ductility of AC-3 is smaller than that of AC-2. Therefore, ultimate load and initial stiffness are increased with increasing prestress and stiffness is decreased with increasing prestress. Ultimate load and initial stiffness of A-1, AC-1 are larger than that of N-1 due to chemical prestress of ASR. Stiffness of AC-1 is smaller than that of A-1. Bond strength between concrete and reinforcement of AC-1 are decreased compared with A-1due to corrosion of reinforcement.

4.3 Strain of the shear reinforcement

Shear reinforcement of AC-2 has a fractured anchorage that is corroded. Therefore, Bond strength between concrete and shear reinforcement of AC-2 are decreased due to corrosion of reinforcement. Strain of AC-2 is smaller than that of A-2 due to decreasing the performance of the shear reinforcement.

When specimen has a fractured anchorage under the condition of the shear reinforcement due to ASR, if development length of shear reinforcement is satisfied to shear crack, shear reinforcement is performed effectively. However, when specimen has a fractured anchorage and is corroded due to combined deterioration of ASR and corrosion, performance of the shear reinforcement is decreased

4.4 Shear crack width

Shear crack width of AC-1 is smaller than that of N-1 due to chemical prestress of ASR. Shear crack width of AC-2 is larger than that of AC-1 and A-2. In the case of AC-2, the performance of the shear reinforcement is decreased compared with AC-1 due to fractured anchorage under the condition of the shear reinforcement. Bond strength between concrete and shear reinforcement of AC-2 are decreased due to corrosion of shear reinforcement. Therefore, shear crack width of AC-2 is larger than that of A-2 due to decreasing the performance of the shear reinforcement.

5 CONCLUSION

The main conclusions obtained from this study are as follows:

(1) In the case of combined deterioration specimen, crack width is increased in the surface concrete on the position of longitudinal reinforcement due to corrosion of reinforcement.

(2) In the case of ASR specimen, shear cracking did not occurred clearly. The shear force carried by concrete is increased due to the chemical prestress of ASR.

(3) In the case of AC-2 and AC-3, shear cracking occurred clearly compared with A-2 and A-3. The bond strength between shear reinforcement and concrete is decreased due to corrosion of shear reinforcement. Therefore, the performance of the shear reinforcement is decreased.

(4) When specimen has a fractured anchorage under the condition of the shear reinforcement due to ASR, if development length of shear reinforcement is satisfied to shear crack, shear reinforcement is performed effectively. However, when specimen has a fractured anchorage and is corroded due to combined deterioration of ASR and corrosion, performance of the shear reinforcement is decreased.

6 REFERENCES

[1] T.Miyagawa, K.Seto, K.Sasaki, Y.Mikata, K.Kuzume and T.Minami (2006): Fracture of Reinforcing Steels in Concrete Structures Damaged by Alkali-Silica Reaction-Field Survey, Mechanism and Maintenance-, Journal of Advanced Concrete Technology, Vol.4, No.3, pp.1-17, Japan Concrete Institute

[2] K.Seto, T.Nishizono, Y.Mikata, S.Maeda and T.Miyagawa (2004): Maintenance for ASR Damaged Road Viaduct, Proceedings of the 12th International Conference on Alkali-Aggregate Reaction in concrete, Beijing,Vol.2, pp.1277-1282, ICAAR,
[3] P.E. Regan. and I. L. Kennedy Reid. (2004): Shear strength of RC beams with defective stirrup anchorages, Magazine of Concrete Research, Vol.56, No.3, pp.159-166
[4] K.Inamasu, Y.Takahashi, Y.Mikata and S.Inoue(2009): Effects of Rupture of Stirrups Due to ASR on Load Carrying Behaviour of Reinforced Concrete Beams, Proc. of the Japan concrete institute, Vol.31, No.1, pp.1255-1260(in Japanese)
[5] Y.Mikata, S.Maeda, Y.Hatano and S.Inoue(2008): Effect of fractured anchorage of shear reinforcements on loading capacity of PC beams, Proceedings of the 13th International Conference on Alkali-Aggregate Reaction in concrete, Trondheim Norway, ICAAR
[6] JSCE(2007): Standard Specification for Concrete Structures 2007, Design(in Japanese)

TABLE 1: Properties of concrete

Series	N	AC	
Curing day(day)	28	28	1088
Compressive strength f'_c (N/mm²)	46.5	50.4	33.8
Tensile strength f_t (N/mm²)	3.49	4.24	2.25
Bending strength f_b (N/mm²)	5.09	6.96	3.09
Elastic modulus E_c (kN/mm²)	27.3	34.0	22.2

TABLE 2: Mix proportion of concrete

*1 Series	G_{max} (mm)	Slump (cm)	W/C (%)	Air (%)	s/a (%)	Unit weight (kg/m³) W	C	*2 S S_n	*2 S S_r	*3 G G_n	*3 G G_r	NaCl	*4 A (cc)
N	20	8	45.5	3.0	44.1	178	391	746	0	1026	0	0	3.91
A, AC	25	8	45.5	3.0	41.1	163	358	356	365	550	572	11.59	3.58

*1 N: normal concrete, A and AC: ASR concrete
*2 S_n: normal fine aggregate, S_r: reactive fine aggregate
*3 G_n: normal coarse aggregate, G_r: reactive coarse aggregate
*4 A: air entraining and water reducing admixture

TABLE 3: Crack densities of specimens

Specimens	Crack densities (mm/mm²) L	M	H	Σ
A-1	0.0140	0.0103	0.0000	0.0243
A-2	0.0194	0.0079	0.0004	0.0277
A-3	0.0116	0.0135	0.0000	0.0251
A-4	0.0139	0.0109	0.0001	0.0249
AC-1	0.0246	0.0059	0.0003	0.0308
AC-2	0.0255	0.0061	0.0016	0.0332
AC-3	0.0247	0.0035	0.0007	0.0289
AC-4	0.0241	0.0021	0.0014	0.0276

TABLE 4: Mechanical properties of corroded reinforcing bars

Specimens	reinforcing bars	The ratio of corrosion weight loss (%)	*1 Yield strength (N/mm²)	*1 Elastic modulus (kN/mm²)
AC-1	No.1	1.53	329	200
	No.2	0.96	330	189
AC-2	No.1	1.57	325	202
	No.2	1.49	329	181
AC-3	No.1	1.46	327	200
	No.2	1.72	341	202
AC-4	No.1	0.84	315	190
	No.2	0.50	320	195

*1 Corroded longitudinal reinforcement was taken out of RC beam after the loading test. Yield strength and elastic modulus is calculated by experimental values using nominal cross sectional area.

TABLE 5: Details of test specimens and results of loading tests

Series	Specimens	Concrete type	Shear reinforcement		Introduced prestress σ_{ct}	*2 Ultimate flexural capacity (cal.)	Ultimate shear capacity (cal.)			Ultimate load capacity (mea.)	*6 Failure mode
			*1 Condition	Spacing (mm)	(N/mm²)	P_{ub} (kN)	*3 V_c (kN)	*4 V_s (kN)	*5 P_{us} (kN)	P_u (kN)	
N	N-1	Sound	Sound	150	2	206.2	33.6	30.8	128.8	191.8	FT
A	A-1	ASR	Sound	150	2	140.7	27.1	30.8	115.9	215.3	FT
	A-2		Fractured	150	2	140.7	27.1	30.8	115.9	213.8	FT
	A-3		Fractured	150	4	150.8	28.7	30.8	119.0	189.8	FT
	A-4		Fractured	100	2	140.6	27.1	46.2	146.7	218.7	FT
AC	AC-1	ASR + CORROSION	Sound	150	2	173.5	32.6	30.8	126.8	221.5	FT
	AC-2		Fractured	150	2	173.8	32.7	30.8	127.1	215.6	FT
	AC-3		Fractured	150	4	184.7	35.6	30.8	132.9	221.1	FT
	AC-4		Fractured	100	2	173.9	33.1	46.2	158.6	207.6	FT

*1 Fractured: fractured anchorage of shear reinforcement (stirrup)
*2 Values calculated by the fiber model
*3 Calculated shear capacity contributed by concrete (based on JSCE Standard Specification [6])
*4 Calculated shear capacity contributed by shear reinforcement (based on JSCE Standard Specification [6])
*5 Calculated ultimate shear capacity ($P_{us}=2(V_c+V_s)$)
*6 FT: flexural tension failure

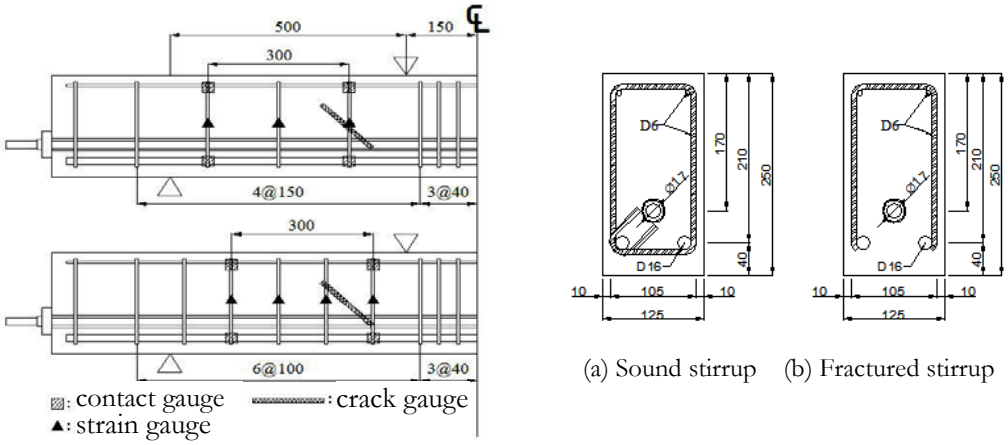

FIGURE 1: Dimensions of specimens and loading condition

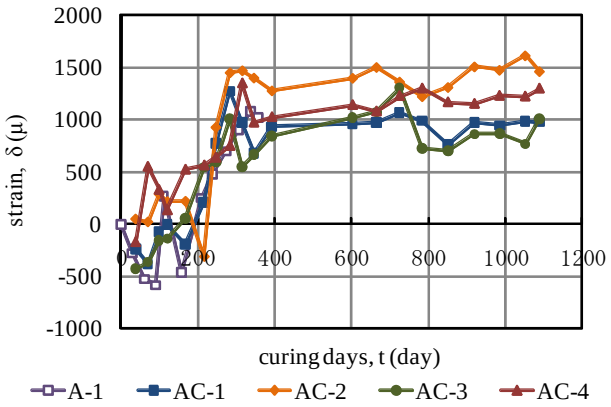

FIGURE 2: Axial strain of ASR expansion

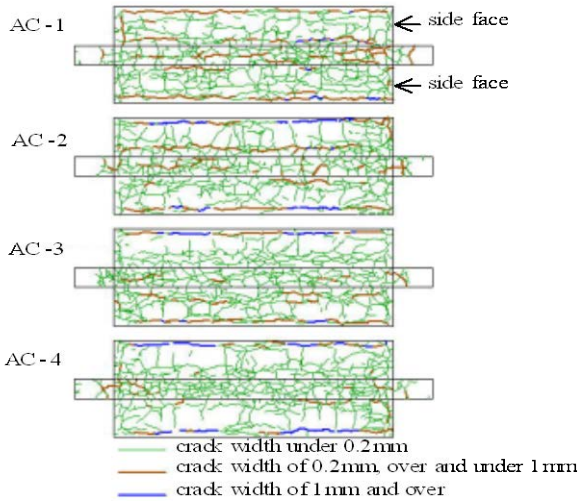

FIGURE 3: Condition of crack before loading tests

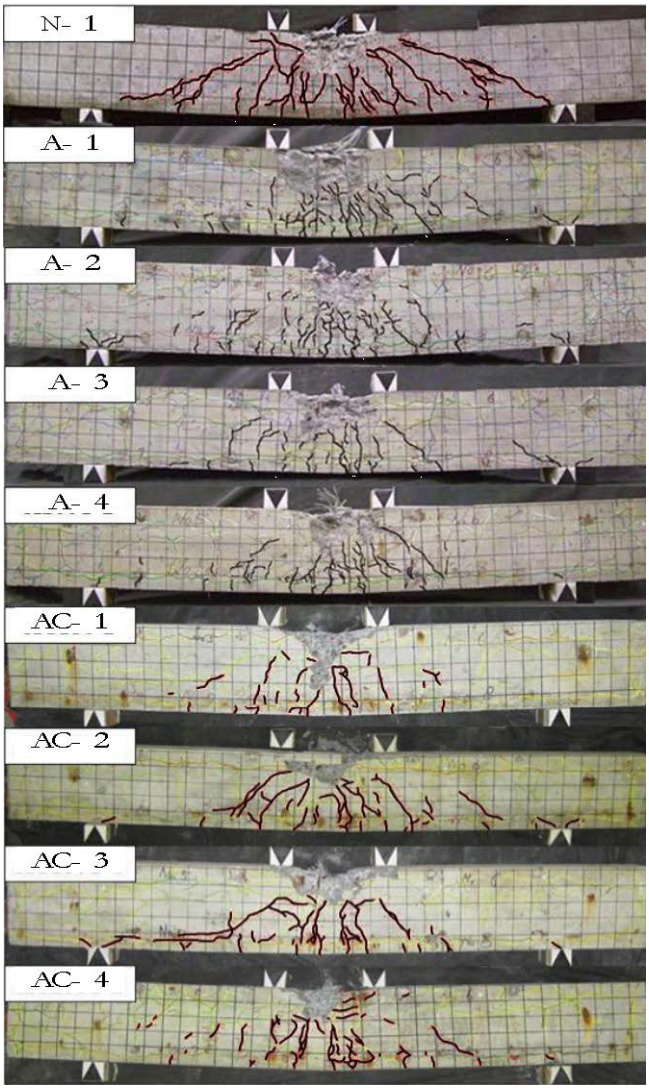

FIGURE 4: Final failure mode

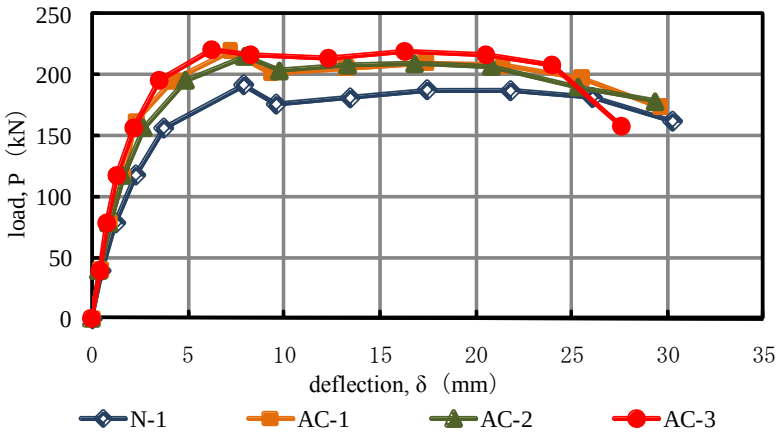

FIGURE 5: Relationship between load and deflection(AC-series and N-1)

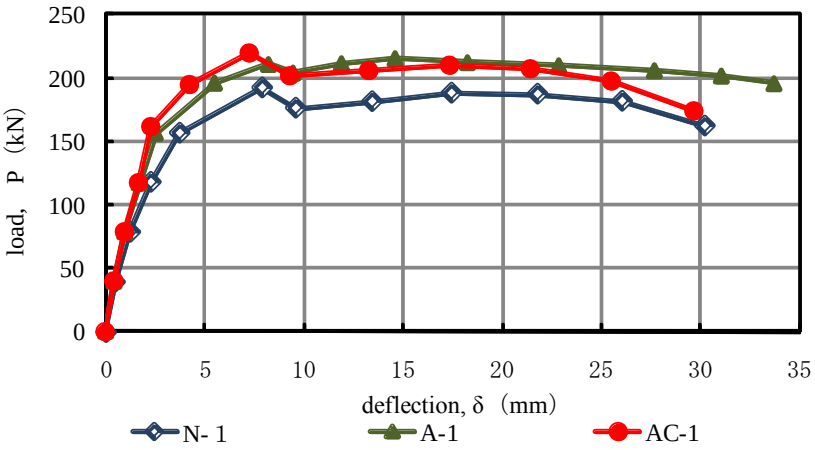

FIGURE 6: Relationship between load and deflection(N-1, A-1, AC-1)

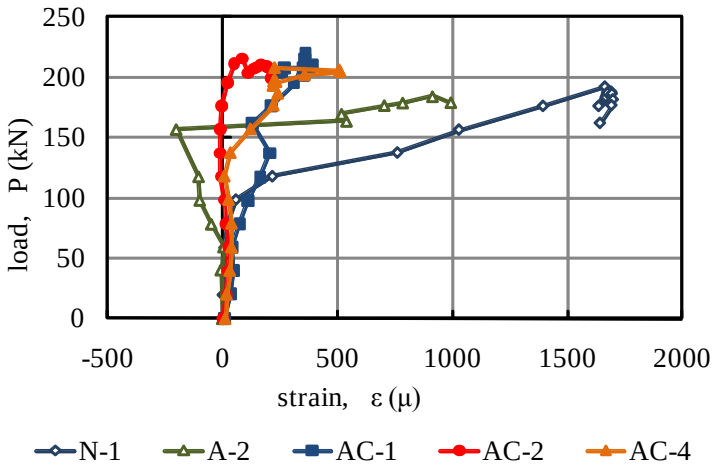

FIGURE 7: Relationship between load and strain of shear reinforcement

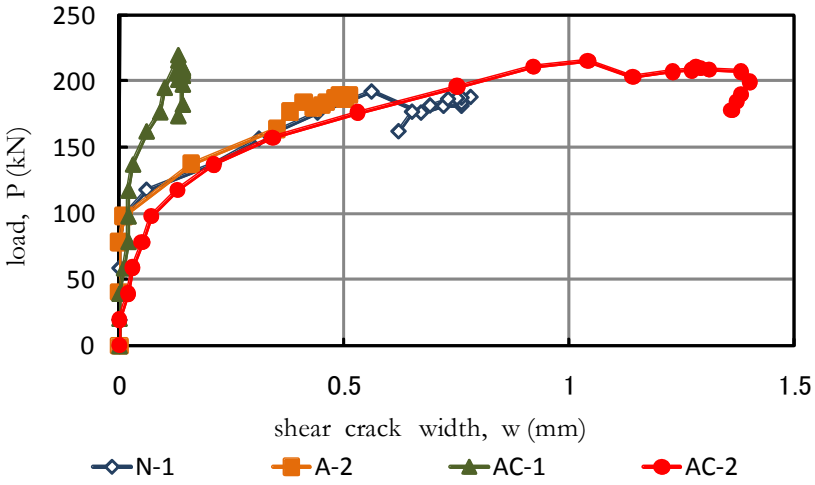

FIGURE 8: Relationship between load and shear crack width